Journal of Chromatography, 134 (1977) 1–24
© Elsevier Scientific Publishing Company, Amsterdam — Printed in The Netherlands

CHROM. 9776

THE ELECTROLYTIC CONDUCTIVITY DETECTOR AS AN ELEMENT-SELECTIVE GAS CHROMATOGRAPHIC DETECTOR

BRIAN E. PAPE*

Department of Pathology, Toxicology Laboratory, School of Medicine, University of Missouri at Columbia, Columbia, Mo. 65201 (U.S.A.)

DONALD H. RODGERS

Tracor Inc., 6500 Tracor Lane, Austin, Texas 78721 (U.S.A.)

and

TIMOTHY C. FLYNN

Department of Pathology, Toxicology Laboratory, School of Medicine, University of Missouri at Columbia, Columbia, Mo. 65201 (U.S.A.)

(Received October 28th, 1976)

SUMMARY

The response and elemental selectivity of the electrolytic conductivity detector (ElCD) to nitrogen-, chlorine-, and sulfur-containing compounds has been investigated as a function of chemical structure, furnace chemistry conditions (*i.e.*, reaction gas, furnace temperature, catalyst, and post-furnace chemical abstractors), and solubilization-and-ionization processes (electrolytic chemistry and electrolytic conductance). The "profiling" of detector response for the gas–liquid chromatographic–ElCD analysis of selected compounds under defined furnace chemistry reaction conditions and electrolytic chemistry included the determination of detector signal to noise ratio, peak tailing, and elemental selectivity. Detector response and conductivity phenomena are discussed in terms of gas-phase furnace chemistry reactions, post-furnace reaction or abstraction processes, and solution-phase ionization and neutralization processes occurring in the conductivity cell.

INTRODUCTION

The application of the principle of electrolytic conductivity detection (ElCD) for the analysis of gas chromatographic effluents was first reported by Piringer and Pascalau[1], and a commercial detector system was subsequently developed by Coulson to allow the selective detection of halogen-, nitrogen-, and sulfur-containing compounds[2,3]. Further studies by Jones and Nickless[4], Dolan and Hall[5], and Lawrence and Moore[6] focused on modifications to the detector system and resulted in improved

* Author to whom inquiries should be directed.

detector sensitivity and elemental selectivity. The instrumental evolution and applications of ElCD have been reviewed by Selucky[7], David[8], and Sevcik[9]. Hall recently constructed an improved microelectrolytic conductivity detector[10] which is now commercially available as the Hall electrolytic conductivity detector (HECD)[11].

The principle of ElCD operation

Effluent from a gas chromatograph undergoes thermal decomposition under predetermined conditions of furnace temperature, reaction gas, reaction catalyst, and chemical abstractors, and the gas-phase reaction products are then combined with a stream of deionized liquid in a simple gas–liquid contactor. The electrical conductivity of the liquid is continuously measured with an a.c. bridge circuit and auxiliary recorder. Only those components are detected in the gas–liquid chromatographic (GLC) effluent that are decomposed to yield products that are both readily soluble and ionized in the conductivity liquid. Fig. 1 shows the relationship of the principle components of the ElCD system, all of which are contained in a single unit.

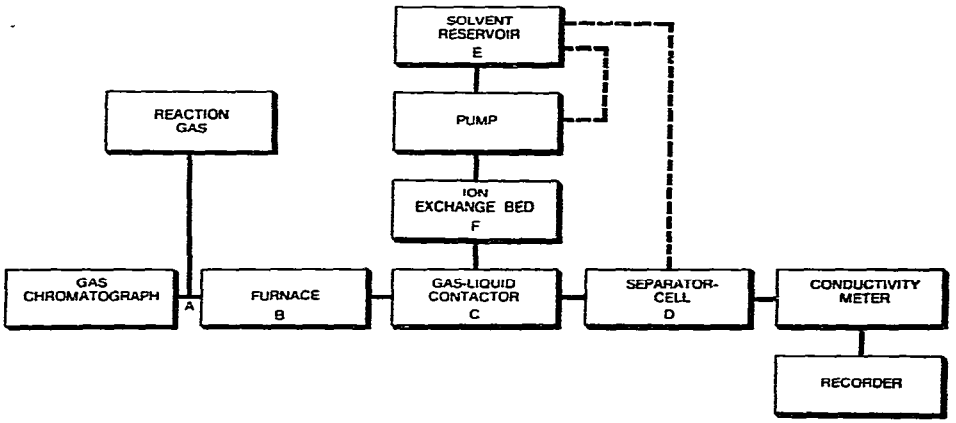

Fig. 1. Block diagram of ElCD.

The pyrolyzer section (A and B) contains the detector furnace, the quartz or nickel reaction tube, and the reaction gas inlet. The cell assembly (C and D) consists of an integrated one-piece PTFE gas–liquid contactor and microconductivity cell made of stainless steel and PTFE. The liquid circulation system (E and F) consists of a glass liquid reservoir, liquid pump, needle valve for flow regulation, and an ion-exchange bed. Components of the conductivity bridge include a fixed-voltage a.c. power supply, current-suppression circuit, and signal attenuator. Conductivity-bridge and electrometer-output controls consist of an attenuator, which selects one of eight binary levels of output signal attenuation; a conductivity range switch, which selects one of seven ranges of full-scale conductivity measurement, from 1–1000 $\mu\Omega^{-1}$; a coarse and fine zero control, which balances the a.c. bridge to allow positioning of the recorder pen; and a display meter selectable for furnace temperature or cell conductivity. Additional components of the detector system include a furnace temperature controller and furnace power and detector power monitors.

Although classified as an electrochemical detector, the principle of ElCD response is different from that of the coulometric or reaction coulometric detectors[8,9], and knowledge of detector variables is critical to the understanding of ElCD response and element selectivity. Thermal decomposition of the GLC effluent is based on the reduction (hydrogen reaction gas), oxidation (oxygen or air reaction gas), or pyrolysis (inert reaction gas) of the organic species at high temperature (usually 800–900°) in a flow-through reaction chamber. Decomposition may involve either catalytic (commonly quartz reaction tube and Ni catalyst, or Ni reaction tube) or non-catalytic conditions (quartz reaction tube). The particular mode of decomposition may be referred to as the "furnace chemistry". The reaction products obtained depend on the molecular structure, furnace chemistry mode, and the use of post-furnace abstractors that trap acidic or basic products. Solubilization and ionization of the reaction products (*e.g.*, NH_3, HCl, Cl_2, S_xO_x, etc.) at the gas–liquid contactor may be referred to as "cell chemistry". Cell chemistry is based on effective gas–liquid contact and separation, on ionization processes, and the use of reactive solutes in the liquid phase. Changes in conductivity attributable to the chemistry of the conductivity solvent and solvent pH, liquid flow-rate, and amplifier setting are often termed "conductance variables". Change in conductance is primarily determined by the concentration of the reaction product(s) in the conductivity cell liquid phase; the dissociation constant(s) (K) of these products in the liquid phase, or the K of the species formed from furnace reaction product(s) and reactive solute(s); and the equivalent ionic conductance [$(\lambda_{+,-}$ (Ω^{-1} cm^2 equiv.$^{-1}$)] of anionic (λ_-) and cationic (λ_+) species in the conductivity solvent[9,12].

Selectivity and sensitivity are determined by a particular combination of furnace chemistry, cell chemistry, and conductance variables[10]. In the reductive mode, H_2S, HCl, NH_3, and hydrocarbons are the major reaction products obtained from Cl-, N-, and S-containing compounds. H_2S has a low dissociation constant in water ($pK_1 = 7.04$) and gives no appreciable response; HCl can be removed by a scrubber such as $Sr(OH)_2$ or $AgNO_3$; and the formation of NH_3 usually requires the use of Ni catalyst. In the oxidative mode, S_xO_x, HCl, CO_2, H_2O, and N_2 are produced from the thermal decomposition of Cl-, N-, and S-containing compounds. The conductivity change produced by CO_2 is low, owing to poor solubilization (short gas–liquid contact time) or the use of an organic conductivity solvent (usually alcohols); H_2O and N_2 give little or no response; sulfur oxides can be removed from the furnace reaction products by using a CaO scrubber; and HCl can also be removed with an acidic scrubber ($AgNO_3$). Consequently, a proper choice of reaction conditions, abstractors, and conductivity liquid allows the highly selective detection of either halogen-, N-, or S-containing compounds.

Selectivity between non-equivalent chlorinated or N-containing compounds may also be realized by the selective optimization of furnace temperature[5] or the proper choice of reaction catalyst[13]. Hall has demonstrated that selectivity for aliphatic *vs.* aromatic chlorine may be realized by the choice of furnace temperature[5], and that urea-based derivatives such as barbiturates do not require Ni catalyst for the reductive conversion (ref. 14). The highly sensitive detection of organic nitrogen with the use of an HCl–ethanol conductivity solvent has also been recommended by Hall[10], where the neutralization reaction ($NH_3 + H_3O^+ \rightarrow NH_4^+ + H_2O$) results in a greater change in total specific conductance ($\Delta C_{sp(tot.)} \approx 37\,\Omega^{-1}$ cm^2

TABLE I

DESCRIPTION OF EICD ELEMENT-SELECTIVE FURNACE CHEMISTRY MODES, FURNACE REACTION CONDITIONS, AND CELL CHEMISTRY

Selectivity: a non-selective mode (N/Cl/S) indicates the absence of an acidic/basic/or CaO post-furnace abstractor; under such conditions, the resin tube (IRN-77 or -78/IRN-150) and liquid pH will determine cell neutralization and ionization processes (see Results). All reaction gas flow-rates were 75 ml/min, unless otherwise noted. Abstractor: fiberfax matrix (20 mg) containing the $Sr(OH)_2$ abstractor was positioned in the post-furnace portion of the quartz reaction tube approximately 0.5 cm in front of the PTFE transfer line [the $Sr(OH)_2$ on fiberfax was obtained from Tracor]. Ion-exchange resins IRN-77, -78, and -150 (Rohm and Haas, Philadelphia, Pa., U.S.A. or Tracor) were soxhlet-extracted for 8 h in methanol followed by 8 h in distilled water prior to use. Stacked bed resins consisted of approximately 70% acidic IRN-77 or basic IRN-78 resin on the pump side and 30% mixed-bed IRN-150 resin on the cell side of the resin tube. Conductivity solvents were isopropanol–distilled water (15:85, v/v) or *n*-butanol (AR grade); liquid flow-rate was 0.5 ml/min unless otherwise noted.

Furnace mode	*Selectivity*	*Reaction gas*	*Reaction catalyst*	*Abstractor*	*Resin tube (pump-side/cell-side resin)*	*Conductivity solvent*	*pH*
Pyrolytic	N	He	—*	$Sr(OH)_2$	IRN-78/IRN-150	Isopropanol–water	7.5–8.0
	Cl	He	—	Acid**	IRN-77/IRN-150	*n*-Butanol	6.0–6.5
Catalytic–pyrolysis	N	He	Ni***	$Sr(OH)_2$	IRN-78/IRN-150	Isopropanol–water	7.5–8.0
	Cl	He	Ni***	Acid**	IRN-77/IRN-150	*n*-Butanol	6.0–6.5
Reductive	N	H_2	—	$Sr(OH)_2$	IRN-78/IRN-150	Isopropanol–water	7.5–8.0
	Cl	H_2	—	Acid**	IRN-77/IRN-150	*n*-Butanol	6.0–6.5
Catalytic–reductive	N	H_2	Ni***	$Sr(OH)_2$	IRN-78/IRN-150	Isopropanol–water	7.5–8.0
	Cl	H_2	Ni***	Acid**	IRN-77/IRN-150	*n*-Butanol	6.0–6.5
Oxidative		O_2	—	—	IRN-77/IRN-150	*n*-Butanol	6.0–6.5
Catalytic–oxidative		O_2	Ni***,§	—	IRN-77/IRN-150	*n*-Butanol	6.0–6.5

* Empty quartz reaction tube, 16 cm × 4 mm I.D. (Tracor).

** The boric acid abstractor employed by Hailey *et al.*[17] was not used to trap NH_3.

*** Approximatley 50 cm of fine nickle wire (Tracor) was coiled into a 3-cm length and positioned in the quartz reaction tube, in the center of the furnace heating zone.

§ Empty 201 or 205 nickel reaction tube, 0.126/0.1261 in. O.D. × 0.0232/0.02345 in. wall, lot No. 2435 (Uniform Tubes, Collegeville, Pa., U.S.A.).

equiv.$^{-1}$ in ethanol[12]) compared to the solubilization and partial ionization of NH_3 at pH > 7 [$NH_3 + H_2O \rightarrow NH_4^+ + OH^-$; $pK_b = 4.76$ (ref. 4); λ_+ $NH_4^+ \approx 19.6$, λ_- $OH^- \approx ?\Omega^{-1}$ cm^2 equiv.$^{-1}$ in ethanol[12]]. Moreover, dilute HCl conductivity solvents have been used to differentiate Cl- and N-containing compounds detected in the non-selective catalytic-reductive mode[4]. Differentiation is based on the decrease in $C_{sp(tot.)}$ due to an NH_3 neutralization process, as opposed to the increase in $C_{sp(tot.)}$ caused by simple HCl ionization (λ^0 or limiting equivalent conductance for NH_4^+, H^+, Cl^-, and OH^- in water $\approx$ 73.5, 349.8, 76.4, and 198.6 Ω^{-1} cm^2 equiv.$^{-1}$, respectively[12]). By analogy, the selective enhancement of ElCD response to sulfur (as H_2S) in the reductive mode may be realized by using a reactive solute in the conductivity solvent[4]. Increased sensitivity is based on the rapid oxidation of H_2S in dilute acid solution containing iodine ($H_2S + I_2 \leftrightharpoons 2H^+ + 2I^- + S$), with $\Delta C_{sp(tot.)} \approx 850\,\Omega^{-1}$ cm^2 equiv.$^{-1}$ of H_2S oxidized in aqueous solution (pK_a HI ≈ 0.8)[12].

The ElCD represents a powerful analytical tool. Surprisingly, it has recieved relatively limited attention, in part due to only the recent introduction of an integrated micro-ElCD system[10], and in part due to limited use in the detection of N- and S-containing compounds. An understanding of the varied applications of selected ElCD furnace chemistry modes and the principles of electrolytic conductance phenomena can only result in a more qualified judgement of the best application of the ElCD to the analytical problem. To this end, we wish to discuss the selectivity of the detector system and the chemical and electrochemical basis of the conductivity processes.

MATERIALS

Gas chromatograph and detector

The GLC–ElCD analyses were done on a Model MT-222 gas chromatograph equipped with a Model 310 Hall ElCD (Tracor, Austin, Texas, U.S.A.). The conventional ElCD reaction-gas inlet was modified with two nupro metering valves and a by-pass valve to a soap-bubble flowmeter, allowing convenient switching between reaction-gas sources and measurement of reaction-gas flow. Furnace chemistry, cell chemistry, and relevant conductance variables for the ElCD element-selective modes are summarized in Table I. Unless otherwise noted, ElCD analyses performed in a particular "Furnace mode" are adequately described by noting "Selectivity" (refer to Table I).

GLC columns and column packings

The GLC packings are denoted as follows. The 3% OV-17 packing contained 30 g of OV-17 per kg of support (100–120 mesh Gas-Chrom Q), and the 2.5% SE-30 packing 25 g of SE-30 per kg of support (80–100 mesh Chromosorb W AW DMCS (Applied Science Labs., State College, Pa., U.S.A.). All GLC columns were glass, approximately 180 cm $\times$ 2 mm I.D.

Chemicals

Compounds used in these studies are summarized in Table II.

TABLE II

NOMENCLATURE, STRUCTURAL CHEMISTRY, AND GLC RETENTION INDICES OF SELECTED COMPOUNDS AND RELATIVE STANDARDS

Retention indices (R.I.) for phenothiazines, diphenylmethanes, tricyclic antidepressants and barbiturates on SE-30 liquid-phase were obtained from Moffat[38] and confirmed as correct to within ±25 units on a 2.5% SE-30 column (see Materials). R.I. for barbiturates on OV-17 liquid-phase were obtained from Kazyak and Permisohn[39]. R.I. for the relative standards were determined on a 2.5% SE-30 and a 3% OV-17 column (see Materials).

Chemical class	*Generic name*	*Chemical name*	*Substituent**	*R.I.*	
				OV-17	*SE-30*
Phenothiazines					
R_{10} unsubstituted	Phenothiazine (I)	Phenothiazine	H		2010
	2-Chlorophenothiazine (II)	2-Chlorophenothiazine	Cl		1975
R_{10} propyl and *s*-butyl dialkylamino substituted	Promazine hydrochloride (III)	10-(3-Dimethylaminopropyl)phenothiazine	H		2295
	Chlorpromazine hydrochloride (IV)	2-Chloro-10-(3-dimethylaminopropyl)-phenothiazine	Cl		2440
	Trimeprazine tartrate (VI)	10-(3-Dimethylamino-2-methylpropyl)-phenothiazine	H		2320
	Methotrimeprazine	(−)-10-(3-Dimethylamino-2-methylpropyl)-2-methoxyphenothiazine	OCH_3		2515
R_{10} alkyl piperidyl and pyrrolidinyl substituted	Thioridazine hydrochloride (VIII)	10-[2-(1-Methylpiperid-2-yl)ethyl]-2-methylthiophenothiazine	SCH_3		3110
	Mesoridazine besylate (IX)	2-Methylsulphinyl-10-[2-(1-methylpiperid-2-yl)-ethyl]phenothiazine	O ↑ SCH_3		
	Methdilazine hydrochloride (X)	10-(1-Methylpyrrolidin-3-ylmethyl)-phenothiazine	H		2470
R_{10} propyl piperazine substituted	Prochlorperazine maleate (XI)	2-Chloro-10-[3-(4-methylpiperazin-1-yl)propyl]-phenothiazine	Cl		2935
	Trifluoperazine hydrochloride (XII)	10-[3-(4-Methylpiperazin-1-yl)propyl]-2-trifluoromethylphenothiazine	CF_3		2680
	Thiethylperazine maleate (XIII)	2-Ethylthio-10-[3-(4-methylpiperazin-1-yl)-propyl]phenothiazine	SCH_2CH_3		3260
	Fluphenazine hydrochloride (XIV)	10-{3-[4-(2-Hydroxyethyl)piperazin-1-yl]-propyl}-2-trifluoromethylphenothiazine	CF_3		3045
Phenothiazine "isosteres"	Chlorprothixene (B)	*cis*-2-Chloro-9-(3-dimethylaminopropyl-idene)-thioxanthene	Cl		2510

Diphenylmethanes					
	Chlorcyclizine hydrochloride (A)	(±)-1-(*p*-Chlorodiphenylmethyl)-4-methyl-piperazine	Cl		2215
	Hydroxyzine hydrochloride (C)	1-(*p*-Chlorodiphenylmethyl)-4-[2-(2-hydroxy-ethoxy)-ethyl]*piperazine*	Cl		2840
	Buclizine hydrochloride (D)	4-(*p*-Chlorodiphenylmethyl)-1-(*p-tert.*-butylbenzyl)-piperazine	Cl		3285
Tricyclic antidepressants					
	Amitriptyline hydrochloride (I)	10,11-Dihydro-5-(3-dimethylaminopropyl-idene)-5H-dibenzo[*a,d*]cycloheptene	3^0		2200
	Nortriptyline hydrochloride (II)	10,11-Dihydro-5-(3-methylaminopropyl-idene)-5H-dibenzo[*a,d*]cycloheptene	2^0		2215
	Imipramine hydrochloride (III)	5-(3-Dimethylaminopropyl)-10,11-dihydro-5H-dibenz[*b,f*]azepine	3^0		2220
	Desipramine hydrochloride (IV)	5-(3-Methylaminopropyl)-10,11-dihydro-5H-dibenz[*a,f*]azepine	2^0		2260
	Protriptyline hydrochloride (V)	5-(3-Methylaminopropyl)-5H-dibenzo[*a,d*]-cycloheptene	2^0		2230
	Doxepin hydrochloride (VI)	11-(3-Dimethylaminopropylidene)-6,11-dihydro-dibenz[*b,e*]oxepin	3^0		2275
Barbiturates					
	Butabarbital (I)			1955	1655
	Amobarbital (II)			1985	1725
	Pentobarbital (III)			2030	1750
	Secobarbital (IV)			2070	1780
	Thiopental (V)			2185	1850
	Thiamylal (VI)			2240	1890
Relative standards					
	C_{18} Hydrocarbon (I)	*n*-Octadecane		1800	1800
	C_{19} Ketone (II)	2-Nonadecanone		2210	2090
	C_{21} Alcohol (III)	1-Eicosanol		2385	2270
	C_{21} Methyl ester (IV)	Eicosanoic methyl ester		2430	2305
	C_{21} Hydroxy methyl ester (V)	2-Hydroxyeicosanoic methyl ester		2585	2435
	C_{18} Methylsulfonate (VI)	Octadecylmethanesulfonate		2770	2505
	Caffeine (VII)			2265	1815
	Azobenzene (VIII)				
	Thioxanthine-9-one (IX)				
	Anthracene (X)				

* Substituents of phenothiazines are R_2 substituents; of diphenylmethanes R_3 substituents; of tricyclic antidepressants 2^0 or 3^0 amines.

METHODS

Determination of ElCD response characteristics

Detectability. The minimum detectable quantity (MDQ) for a particular compound was defined as the weight or molar quantity of the compound or "reactive" element (*i.e.*, Cl, N, S) which resulted in a detector signal to noise ratio of greater than 2:1 when injected "on-column" and analyzed under defined chromatographic and detector conditions (see Results and Discussion). The detector signal was measured in terms of peak height or percent of full-scale deflection (f.s.d.), while noise was defined as the observed short-term noise and was measured as average peak-to-valley height or percent of f.s.d. The lower limit of detectability (LLD) for a particular "on-column" GLC–ElCD analysis was defined as the observed detector signal to noise ratio divided into the sample weight, and is accompanied by a description of GLC and ElCD parameters[8].

GLC–ElCD selectivity and elemental equivalence. The relative response of the ElCD when operated in an element-selective mode is discussed in terms of detector variables (Table I), the reaction chemistry of the compound of interest and the relative standard (Table II), and the experimental conditions (see Results and Discussion). ElCD molar selectivity ratios for a compound of interest, A, *vs.* a relative standard, B, were calculated according to eqn. 1:

$$\text{ElCD molar selectivity ratio}_{A/B} = \frac{\text{peak area}_A}{\text{peak area}_B} \cdot \frac{[B]}{[A]} \cdot \frac{\text{elect. attn.}_A}{\text{elect. attn.}_B} \quad (1)$$

where detector responses to A and B are expressed as peak area_A and peak area_B, respectively, [A] and [B] refer to the molar quantity injected on-column, and elect. attn. refers to the respective conductivity range × attenuation used for a particular analysis. Eqn. 1 was easily modified to obtain ElCD element-selectivity ratios for A *vs.* B:

$$\text{ElCD N/C selectivity ratio}_{A/B} = \frac{\text{peak area}_A}{\text{peak area}_B} \cdot \frac{[B]}{[A]} \cdot \frac{\text{elect. attn.}_A}{\text{elect. attn.}_B} \cdot \frac{(C)_B}{(N)_A} \quad (2$$

where, using the ElCD N-selectivity of azobenzene *vs. n*-octadecane as the example, $(C)_B$ and $(N)_A$ refer to the number of carbons in *n*-octadecane and the number of nitrogens in azobenzene, respectively. Assuming a high N/C selectivity ratio, the contribution of the carbon content of A was disregarded. This eqn. 2 then represents the ElCD selectivity for NH_3 *vs.* CH_4, when the ElCD was operated in the N-selective catalytic–reductive mode and complete reductive pyrolysis and 100% product throughput from furnace-to-conductivity cell were assumed. The quantitative determination of relative elemental contributions to ElCD response under non-selective conditions (refer to Table I) was more complex and is discussed in the Results and Discussion.

Variance from an equivalent detector response for chemical analogs containing the same reactive element (*e.g.*, N-containing A *vs.* A') was estimated from eqn. 3.

$$\text{ElCD N-equivalence}_{A/A'} = \frac{\text{peak area}_A}{\text{peak area}_{A'}} \cdot \frac{[A']}{[A]} \cdot \frac{\text{elect. attn.}_A}{\text{elect. attn.}_{A'}} \cdot \frac{(N)_{A'}}{(N)_A} \quad (3)$$

ElCD response to the carbon content of A and A′ was not considered when the N/C element-selectivity ratios for A and A′ *vs.* *n*-octadecane were $> 10^3$.

If differences in the GLC throughput of A and A′ contributed to a non-equivalent ElCD response to A *vs.* A′, a correction factor$_{FID}$ based on the GLC–flame ionization detection (FID) analysis of A and A′ under chromatographic conditions equivalent of GLC–ElCD analysis was used to adjust the ElCD N-equivalent response (eqn. 4):

$$\text{ElCD N-equivalence}_{A/A'}\text{ (corr. FID)} = \\ = [\text{ElCD N-equivalence}_{A/A'}] \Big/ \left[\frac{\text{peak area}_A}{\text{peak area}_{A'}} \cdot \frac{[A']}{[A]} \cdot \frac{(C)_{A'}}{(C)_A} \cdot \frac{\text{elect. attn.}_A}{\text{elect. attn.}_{A'}}\right]_{FID} \quad (4)$$

where A and A′ refer to the selected chemical analogs, (N) and (C) refer to the respective number of nitrogens and carbons per molecule, and [A] and [A′] refer to the molar quantity of A and A′ injected on-column. When A and A′ were equimolar and were analyzed under equivalent GLC and electrometer conditions, eqn. 4 was simplified to eqn. 5.

$$\text{ElCD N-equivalence}_{A/A'}\text{ (corr. FID)} = \\ = \left[\frac{\text{peak area}_A}{\text{peak area}_{A'}} \cdot \frac{(N)_{A'}}{(N)_A}\right]_{ElCD} \cdot \left[\frac{\text{peak area}_{A'}\,(C)_A}{\text{peak area}_A\,(C)_{A'}}\right]_{FID} \quad (5)$$

The correction factor assumed that equivalent GLC conditions in FID and ElCD analyses resulted in equivalent loss factors; that FID carbon-equivalence for structural analogs was close to unity and a good measure of GLC throughput: and that there was no difference between GLC–FID and GLC–ElCD loss factors due to differences in injector port or post-column decomposition processes.

Peak tailing. Peak tailing, T, was expressed as $T = \omega/h$ where ω was the peak width at a defined fraction of peak height, h.

GLC–ElCD analyses

Substituted phenothiazines and diphenylmethanes. Two microliters of methanolic solutions containing 2×10^{-4} moles/l of selected phenothiazines I–XIV were analyzed by temperature-programmed GLC on 2.5% SE-30 (175° isothermal for 2 min, followed by temperature programming at 8°/min). Injection solvent was vented prior to the reaction furnace and the compounds were detected under defined ElCD parameters (see Table I and Results and Discussion).

Tricyclic antidepressants. Two microliters of equimolar solutions of tricyclics in methanol (*ca.* 100 ng of antidepressant I–VI per 2 μl) were analyzed on 2.5% SE-30 at 205° isothermal column temperature. Injection solvent was vented and the ElCD was operated under defined parameters.

Barbiturates. On-column injections of 2 μl of a methanolic solution containing barbiturate analogs and azobenzene (*ca.* 0.5 μg per μl of I–VI and VIII) were analyzed by temperature-programmed GLC on a 3% OV-17 column (150–250° at 8°/min). The ElCD was operated in the N-selective reductive mode (Table I).

Methaqualone. On-column injections of 100 ng of methaqualone were analyzed on 2.5% SE-30 at an isothermal column temperature of 200°.

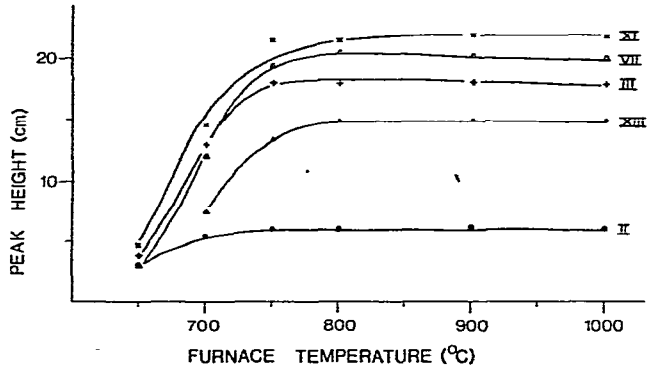

Fig. 2. ElCD furnace temperature profiles of substituted phenothiazines II, III, VII, XI and XIII in the N-selective catalytic-reductive mode.

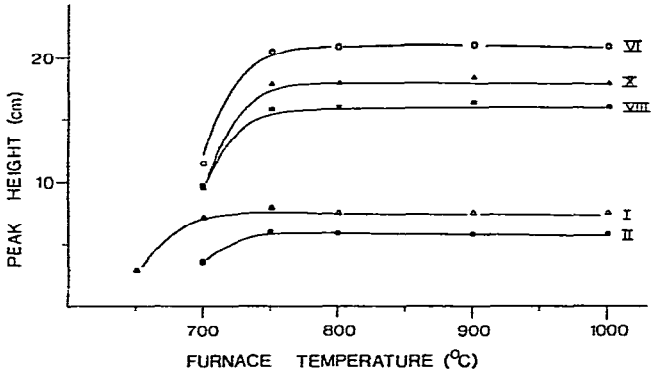

Fig. 3. Profiles for phenothiazines I, II, VI, VIII and X.

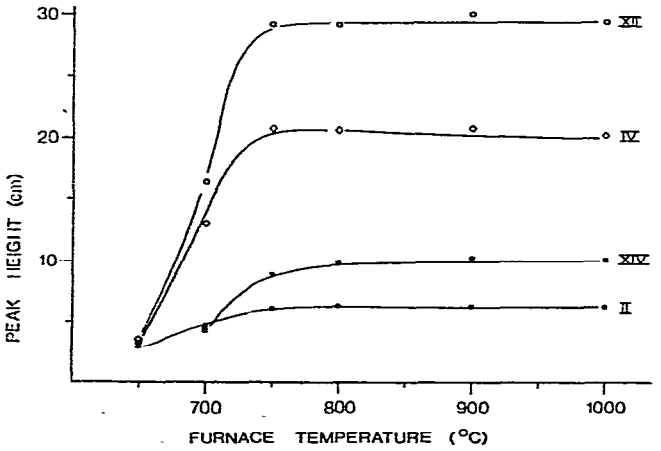

Fig. 4. Profiles for phenothiazines II, IV, XII and XIV.

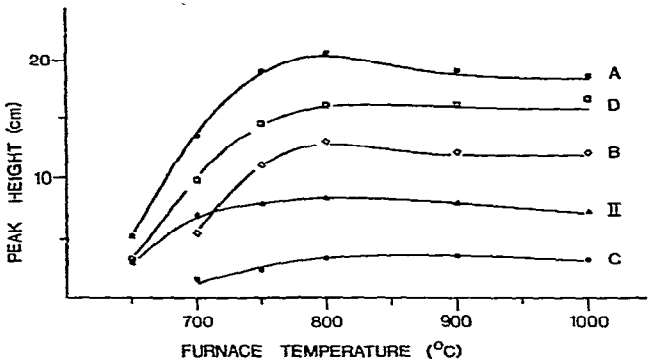

Fig. 5. E1CD furnace temperature profile of selected diphenylmethanes (A, C, D), chlorprothixene (B), and 2-chlorophenothiazine (II) in the N-selective catalytic-reductive mode.

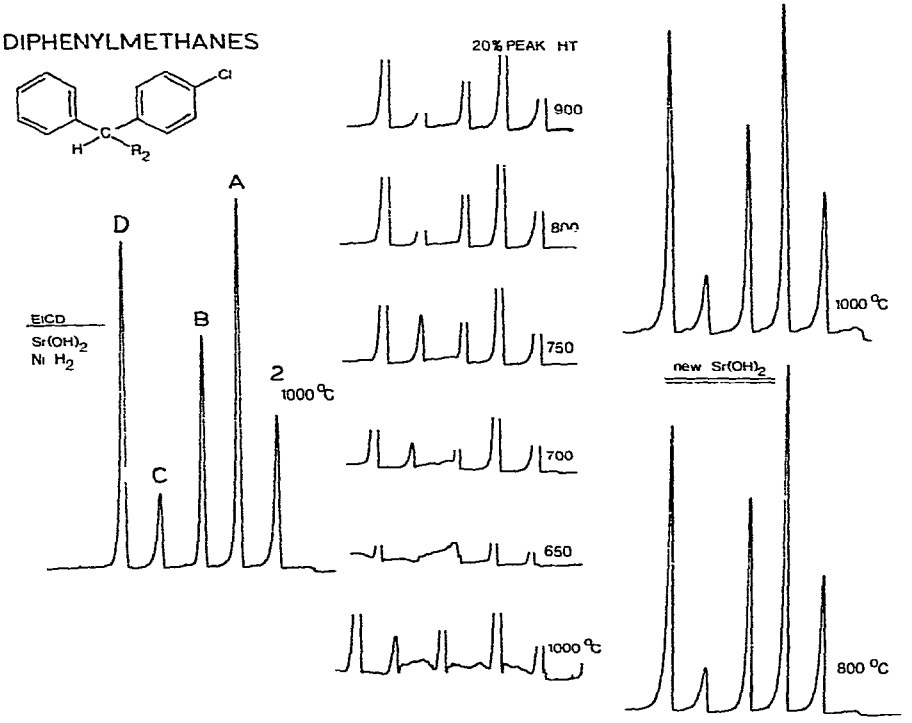

Fig. 6. GLC–E1CD analysis of diphenylmethanes (A, C, D), chlorprothixene (B), and 2-chlorophenothiazine (II) under different furnace temperature and post-furnace abstractor conditions.

Furnace temperature profiles

Furnace temperature profiles for substituted phenothiazines (Figs. 2–4), diphenylmethanes (Fig. 5), and tricyclic antidepressants (Fig. 7) were obtained using the same furnace-and-cell chemistry conditions and temperature sequence. All profiles were determined in the N-selective catalytic-reductive mode; a high-to-low furnace temperature sequence was used to obtain the response data; and significant catalytic

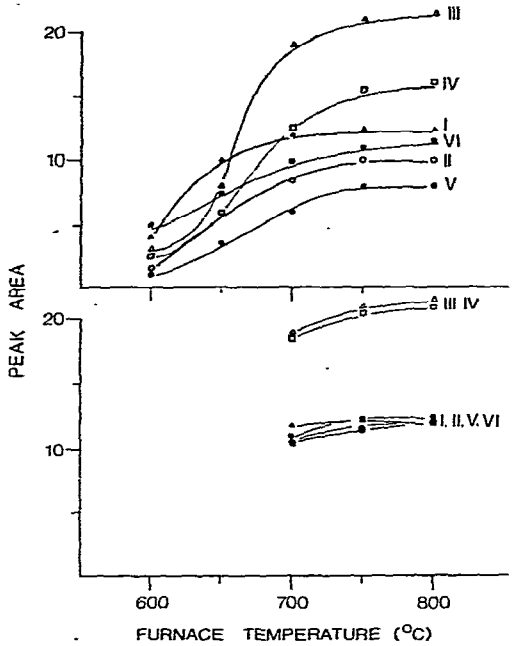

Fig. 7. EICD furnace temperature profiles for tricyclic antidepressants in the N-selective catalytic-reductive mode using uncorrected (top) and corrected (bottom) response data.

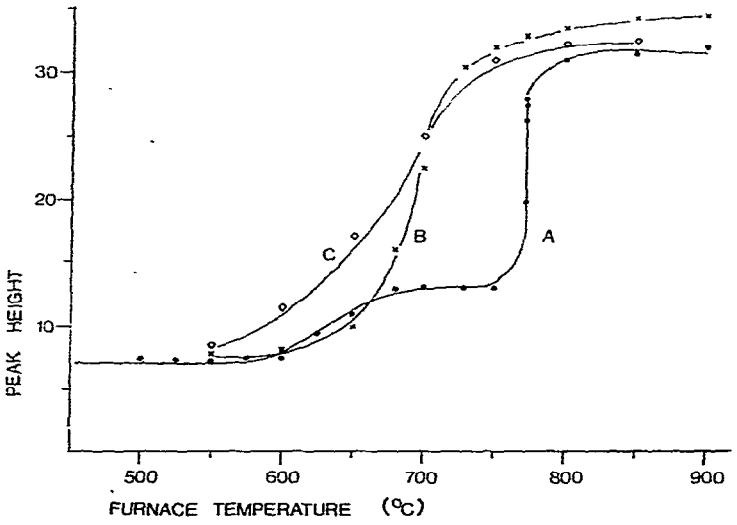

Fig. 8. EICD temperature profiles of imipramine in the N-selective catalytic-reductive mode illustrating differences in catalytic activity. Profile A, 500–900° sequence; B, 550–900° sequence; C, 900–550° sequence.

deactivation did not occur at low furnace temperatures due to column bleed. GLC–ElCD parameters and on-column analyses are discussed above and in Table I.

Temperature- and sequence-dependent furnace chemistry profiles for imipramine (Fig. 8) were obtained using equivalent GLC–ElCD parameters and on-column analysis, but with different furnace temperature sequence patterns (see Results and Discussion). Temperature profiles for "oxidized Ni catalyst deactivation due to column bleed" were obtained under GLC–ElCD conditions identical to those used for phenothiazine temperature profiling (Figs. 2–4); but anomalies were demonstrated to be due to the condition of the catalyst and SE-30 liquid-phase bleed (Results and Discussion, Fig. 9).

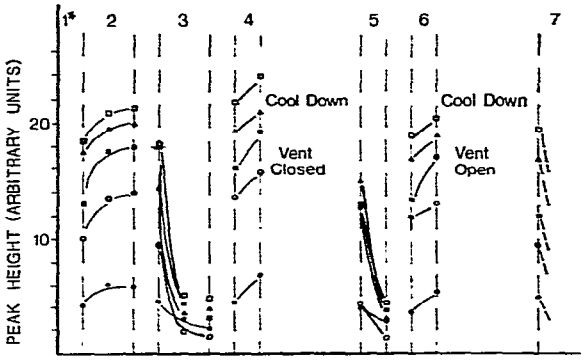

Fig. 9. ElCD catalyst activation–deactivation profiles for phenothiazines II (●), XIII (○), III (■), VI (▲), and XI (□) in the N-selective catalytic-reductive mode. Time-equivalent temperature zones were: 1, 850°; 2, 950°; 3, 650°; 4, 950°; 5, 650°; 6, 950°; and 7, 650° (furnace temperature). Distance within a temperature zone or between temperature zones represents time of temperature equilibration or transition. "Vent closed" indicates that the GLC effluent enters the reaction furnace during cool-down and equilibration, while "vent open" indicates that the GLC effluent is vented prior to the reaction furnace.

Selectivity ratios

Unless otherwise noted, ElCD molar or elemental selectivity ratios were determined *vs.* the on-column injection of 5 μg of relative standard (I–X), and the ratios were calculated according to eqns. 1 and 2.

RESULTS AND DISCUSSION

Substituted phenothiazines

The N-selective analysis of substituted phenothiazines required the use of Ni catalyst and hydrogen reaction gas. Although the chemistry of the R_{10} and R_2 substituents was quite different, ElCD furnace temperature profiles were quite similar (Figs. 2–4).

Even when individual phenothiazines were corrected for their nitrogen content and ElCD response was related to 2-chlorophenothiazine as a common internal standard, wide differences were noted in the uncorrected GLC–ElCD N-equivalent response (eqn. 3; see Table III). Since the GLC of substituted phenothiazines has been shown to suffer from compound loss due to on-column or transfer-line decomposition

PHENOTHIAZINES

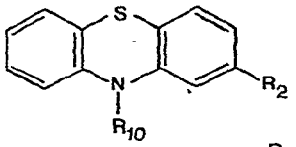

R_{10}		R_2
alkyl dialkylamino	$-N(CH_3)_2$	H
alkyl piperidyl	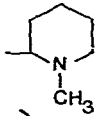	Cl
alkyl pyrrolidinyl	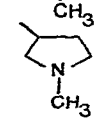	CF_3
alkyl piperazine	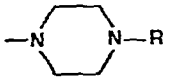	SCH_3
		OCH_3
		SCH_2CH_3

or sorption processes[15], a $correction_{FID}$ factor was determined to reflect the loss of individual phenothiazines due to GLC (eqn. 5). The small variation of corrected response data from an equivalent ElCD nitrogen response (1.0 ± 0.1; refer to Table III) may be due to a real difference in the furnace chemistry of a selected phenothia-

TABLE III

RELATIVE ElCD N-SELECTIVE CATALYTIC-REDUCTIVE RESPONSE TO SUBSTITUTED PHENOTHIAZINES, DIPHENYLMETHANES, AND "MODEL" COMPOUNDS *vs.* 2-CHLOROPHENOTHIAZINE AT 850° FURNACE TEMPERATURE

Furnace temperature: see profiles in Figs. 2–5.

Compound	*N-equivalent response*	
	Uncorrected (eqn. 3)	*$Corrected_{FID}$ (eqn. 5)*
Phenothiazine (I)	1.45	1.04
2-Chlorophenothiazine (II)	1.00	1.00
Promazine (III)	1.44	1.10
Chlorpromazine (IV)	1.32	1.07
Trimeprazine (VI)	1.42	1.05
Methotrimeprazine (VII)	1.38	1.07
Thioridazine (VIII)	1.26	1.05
Mesoridazine (IX)	0.57	0.94
Methdilazine (X)	1.32	1.07
Prochlorperazine (XI)	1.07	0.98
Trifluoperazine (XII)	1.17	0.98
Thiethylperazine (XIII)	1.06	0.99
Fluphenazine (XIV)	0.40	0.90
Chlorprothixene (B)	0.60	0.89
Chlorcyclizine (A)	1.01	1.06
Hydroxyzine (C)	0.40	0.84
Buclizine (D)	0.85	0.97
Thioxanthine-9-one (IX)	$<10^{-3}$	
Anthracene (X)	$<10^{-3}$	

zine relative to 2-chlorophenothiazine (*e.g.*, extent of reductive deamination, or the influence of other reaction products such as HX (X = halogen) or H_2S, or to the nature of the assumption of a true correction factor based on GLC–FID response to the carbon content of individual compounds[15]. Sufficient data were not accumulated to allow the identification of statistically significant differences in detector response.

Differences in the MDQ for substituted phenothiazines are largely a function of a compound's GLC loss factor rather than ElCD sensitivity. Corrected ElCD response data for the on-column injection of 4×10^{-10} moles of phenothiazines demonstrated that the R_2 substituent did not appreciably effect detector response in the N-selective catalytic-reductive mode. An earlier report[16] suggested and LLD for four different phenothiazines equivalent to approximately 10 pg N-content, which is consistent with the manufacturer's specifications[11].

ElCD selectivity ratios for phenothiazines *vs.* relative standards were dependent on at least three factors: (1) furnace temperature; (2) the use of post-furnace $Sr(OH)_2$ abstraction; and (3) the activity of the Ni catalyst (see Table IV). When slightly oxidized Ni catalyst was used, a negative response to 2-nonadecanone in the non-selective catalytic-reductive mode suggested the production of an acidic species, resulting in a neutralization reaction when the pH of the conductivity solvent was >7. A neutralization process was not noted when $Sr(OH)_2$ was used to abstract acidic reaction products.

ElCD response to phenothiazines in the N-selective reductive mode was characterized by *ca.* 100-fold decrease in detector response compared to the catalytic mode, a decreased ElCD selectivity ratio for phenothiazines *vs.* relative standards, and an increase in peak tailing. Detector response in the non-selective catalytic-reductive mode was 75–95% of that obtained in the N-selective mode, and increased peak tailing with halogenated phenothiazines suggested the formation of NH_4X in the post-furnace transfer line[16,17] (refer to *Diphenylmethanes* for further discussion). ElCD analysis in the non-selective catalytic-oxidative mode using Ni wire or Ni tube as the reaction catalyst resulted in a much higher MDQ and LLD due to increased

TABLE IV

ElCD MOLAR SELECTIVITY RATIOS (EQN. 1) FOR SELECTED PHENOTHIAZINES *VS.* RELATIVE STANDARDS (I–IV) UNDER DIFFERENT CONDITIONS OF CATALYTIC ACTIVITY AND POST-FURNACE ABSTRACTION

Ox.Ni refers to slightly oxidized Ni wire (see Results and Discussion); Ni refers to polished Ni wire. Yes and no refer to the presence or absence of $Sr(OH)_2$, respectively (post-furnace abstraction). Relative standards were *n*-octadecane (I), 2-nonadecanone (II), and eicosanoic methyl ester (IV). A negative selectivity ratio (—) indicates a negative detector response due to a neutralization reaction caused by the relative standard.

Phenothiazine	*Molar selectivity vs. relative standard*							
	I				*II*		*IV*	
	Ox.Ni		*Ni*		*Ox.Ni*	*Ni*	*Ox.Ni*	*Ni*
	yes	*no*	*yes*	*no*	*yes* *no*	*yes* *no*	*yes* *no*	*yes* *no*
Phenothiazine (I)	380	280	$>10^4$		340 −280	$>10^4$	280 400	$>10^4$
Methothrimeprazine (VII)	1600	1200	$>10^4$		1500 −1280	$>10^4$	1260 1600	$>10^4$
Methdilazine (X)	1200	850	$>10^4$		1120 −870	$>10^4$	900 1230	$>10^4$
Prochlorperazine (XI)	1800	1200	$>10^4$		1630 −1100	$>10^4$	920 1600	$>10^4$

detector noise, peak tailing, and poor detector response compared to the N-selective catalytic-reductive mode. The catalytic-oxidative mode should yield CO_2, SO_x, and N_xO_x as the major reactive furnace products[9]:

$CO_2 + 3\,H_2O \rightarrow 2\,H_3O^+ + CO_3^{2-}$	H_2CO_3 ($pK_1 = 6.37$, $pK_2 = 10.25$)
$SO_2 + 3\,H_2O \rightarrow 2\,H_3O^+ + SO_3^{2-}$	H_2SO_3 ($pK_1 = 1.81$, $pK_2 = 6.91$)
$SO_3 + 3\,H_2O \rightarrow 2\,H_3O^+ + SO_4^{2-}$	H_2SO_4 ($pK_1 < 1$, $pK_2 = 1.92$)
$N_2O_3 + 3\,H_2O \rightarrow 2\,H_3O^+ + 2\,NO_2^-$	HNO_2 ($pK_a = 3.37$)

Oxides of carbon, sulfur, and nitrogen have a uniformly low gas–liquid solubility compared to NH_3 or HCl[9]. In view of the K value of products and the λ^0 of the H^+ and anionic dissociation products, the relatively low $\Delta C_{sp(tot.)}$ in the oxidative mode compared to the catalytic-reductive mode must be due to poor conversion to product(s) and/or post-furnace reaction or sorption processes resulting in low product throughput.

Diphenylmethanes

The N-selective catalytic-reductive analysis of selected diphenylmethanes, chlorprothixene, and 2-chlorophenothiazine internal standard allowed the selective examination of the influence of heterocyclic and alkylamino substituents on ElCD furnace chemistry processes. Furnace temperature profiles for A–D were similar to those obtained with substituted phenothiazines and suggested no appreciable difference in furnace chemistry requirements for the decomposition of ring nitrogen compared to alkylamino nitrogen (Figs. 2–4 *vs.* 5). Chlorprothixene, an isostere of chlorpromazine in which nitrogen is replaced with a methylene group, exhibited a temperature profile similar to propyl dialkylamino R_{10} substituted phenothiazines and a corrected N-equivalence of *ca.* 1. The conversion of organic N → NH_3 was not related to chemical structure when Ni catalyst and high furnace temperatures were used (Table III).

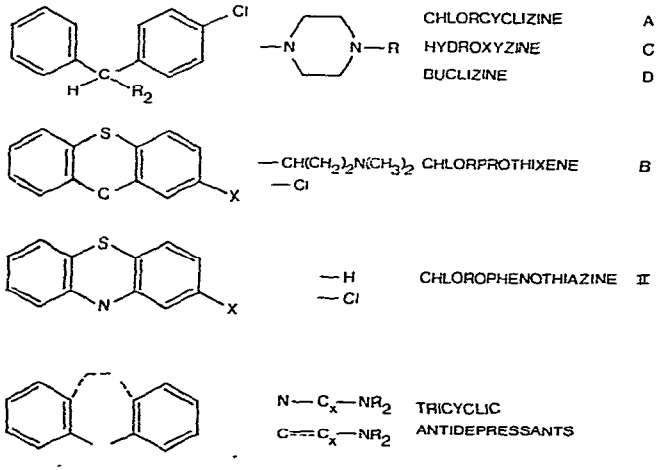

Repeated injections resulted in decreased ElCD response, increased peak tailing, and the appearance of a neutralization → ionization phenomenon (*i.e.*, initial decrease in conductivity followed by an increase in conductivity) (Fig. 6). These

phenomena were documented, and were demonstrated to be the result of: (1) incomplete abstraction of HCl by post-furnace $Sr(OH)_2$; (2) the post-furnace formation of NH_4Cl; and (3) the improper pH of the conductivity liquid.

With incomplete abstraction of HCl, the gas-phase production of NH_4Cl will occur in the post-furnace transfer line and may be detected as a ghost peak or as increased peak tailing. Hailey *et al.*[17] suggested NH_4Cl formation in the analysis of 1,4-benzodiazepin-2-ones, but did not discuss influence on detector response. With inefficient abstraction of HCl, increased ghosting or peak tailing at lower furnace temperatures reflected a shift in furnace chemistry which suggested an increase in the relative production of HCl *vs.* NH_3. Reductive dechlorination is generally viewed as requiring less reactive conditions than reductive deamination[18,19]. The quantitative effect of NH_4Cl formation depends upon a number of factors which include: (1) relative throughput of NH_4Cl to the conductivity cell compared to the throughput of NH_3, *i.e.*, net loss in NH_3 throughput *vs.* net gain in NH_4Cl; (2) the dissociation or ionization constants of NH_4Cl and NH_3 in the conductivity solvent; and (3) the conductance of these dissociation or ionization products.

$$NH_4Cl + H_2O \leftrightharpoons NH_4^+ + Cl^-$$
$$NH_3 + H_2O \leftrightharpoons NH_4^+ + OH^-$$

This is due to the difference in the λ of the ionization products of NH_4Cl *vs.* NH_3 in the conductivity liquid (λ^0 for NH_4^+, Cl^-, and OH^- in water are *ca.* 73.5, 76.35, and 198.6 Ω^{-1} cm^2 equiv.$^{-1}$, respectively[12], resulting in an effective difference of *ca.* 195 Ω^{-1} cm^2 equiv.$^{-1}$ when complete dissociation is assumed at infinite dilution[9].

The neutralization → ionization process involved a two-step electrochemical conductance process:

(1) $NH_3 + H_3O^+ \rightarrow NH_4^+ + H_2O$ ($C_{sp(tot.)}$ decreases)
(2) $NH_3 + H_2O \leftrightharpoons NH_4^+ + OH^-$ ($C_{sp(tot.)}$ increases)

With a neutral or acidic conductivity solvent, a step-1 neutralization process resulted in a decrease in conductivity ($\Delta\lambda^0$ for H^+ *vs.* $NH_4^+ \approx 280\ \Omega^{-1}$ cm^2 equiv.$^{-1}$)[12]. Further introduction of NH_3 resulted in a net increase in liquid conductance due to the ionization of NH_3 in a step-2 process. A negative conductance process on the backside of the GLC peak was a step-1 neutralization process which was observed only when solvent pH was $\leqslant 7$.

Conductance anomalies were not readily predictable or understandable without knowledge of the compound's thermal decomposition process(es), abstractor efficiencies and related post-furnace gas-phase reactions, conductivity solvent pH, and the relation between ionization processes and change in conductance. Remedies to conductance anomalies such as the one illustrated above were usually simple and immediate, involving: (1) an increase in furnace temperature to shift the reaction process to favor the highest production of NH_3 relative to HCl; (2) replacement of the post-furnace chemical abstractor; (3) adjustment of solvent pH by changing the liquid flow-rate through the stacked-bed ion-exchange tube or by introducing trace volumes of nitrogen via the reaction-gas manifold ($N_2 + 3\ H_2 + Ni \rightarrow 2\ NH_3$); or (4) the injection of more material on-column so that any conversion of NH_3 product

via a step 1 neutralization process was small relative to NH_3 available for a step 2 ionization process.

Tricyclic antidepressants

Tricyclics I–VI were analyzed at different furnace temperatures in the N-selective catalytic-reductive mode to obtain uncorrected and corrected temperature profiles (Fig. 7). Corrected$_{FID}$ response factors confirmed that on-column sorption occurred with the secondary alkylamino analogs II, IV, and V[16], and supported the concept of an equivalent response to organic nitrogen under optimum reaction conditions. The temperature profiles for imipramine (III) and desipramine (IV) were quite different from the other tricyclics below 700°; but an understanding of the chemical basis for this difference must await the further elucidation of furnace chemistry mechanisms and product distribution (refer to Specialized applications and studies). The therapeutic concentrations of these tricyclics in plasma have been quantitated using ElCD[16] and thermionic[20] detector systems and, as such, represent an alternative to GLC–mass spectrometry[21].

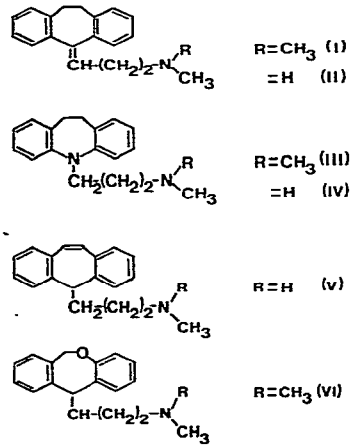

Relation of catalytic activity to furnace temperature profiles

The shapes of ElCD furnace temperature profiles were sometimes affected by differences in the furnace temperature sequence used to obtain the profile of detector response as well as the extent of catalyst deactivation by GLC column bleed or compound. The effect of using different patterns of injection or furnace temperature sequence is demonstrated by different profiles obtained for imipramine in the N-selective catalytic-reductive mode (Fig. 8). The determination of a true temperature profile (*i.e.*, a set of discrete temperature-equilibrated response data using a catalyst of representative activity, where deactivation as a result of previous injection or GLC liquid-phase bleed is insignificant) is unimportant in routine qualitative and quantitative analysis. However, when pattern recognition is used as a means of qualitative identification, catalyst deactivation processes are of great importance[16]. Such pattern recognition, where characteristic changes in detector response are due to changes in detector furnace chemistry, has proven to be of use in the analysis of low-molecular-weight chlorinated volatiles in biological specimens[16,22].

An example of temperature-dependent catalyst deactivation was documented as being due to the use of a partially oxidized Ni catalyst and SE-30 liquid-phase bleed from a poorly conditioned GLC column (Fig. 9). The ability to vent the GLC effluent during the furnace cool-down and equilibration demonstrated that catalyst deactivation may be dependent on furnace temperature; and that furnace temperatures of $> 900°$ may be required in such a case to maintain an acceptable, steady-state level of catalytic activity. Other catalysis research has demonstrated the formation of carbon deposits on Ni catalyst[23], and has shown that catalytic deactivation of a slightly oxidized Ni surface occurs more readily than a polished catalyst[24].

Barbiturates

Because barbiturates poison Ni catalyst, they are routinely detected in the N-selective reductive furnace mode[14,16]. Furnace temperature profiles have been reported by Hall and Risk[14] and Pape[16], and Hall and Risk have reported the direct extraction-GLC–ElCD analysis of barbiturates in plasma at concentrations as low as 0.1 mg/l by using a phosphoric acid-deactivated OV-17 column [on-column injections as low as 1 ng of barbiturate, with a N/C element-selectivity of $>10^6$ (ref. 14)].

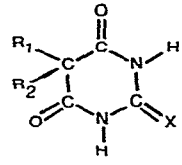

BARBITURATE	R_1	R_2	X
I	CH_3CH_2	$CH_3CH_2CH(CH_3)$	O
II	CH_3CH_2	$(CH_3)_2CHCH_2CH_2$	O
III	CH_3CH_2	$CH_3CH_2CH_2CH(CH_3)$	O
IV	$CH_2{=}CHCH_2$	$CH_3CH_2CH_2CH(CH_3)$	O
V	$CH_2{=}CHCH_2$	$CH_3CH_2CH_2CH(CH_3)$	S
VI	CH_3CH_2	$CH_3CH_2CH_2CH(CH_3)$	S

The GLC–ElCD analysis of equivalent molar weights of thiobarbiturates (V, VI) resulted in a surprisingly low detector response compared to their oxygen analogs (I–IV) (see Fig. 10). Corrected_{FID} N-equivalent response ratios of *ca.* 0.5 for thiobarbiturates *vs.* oxygen analogs were not explained in terms of differences in optimum furnace chemistry conditions since the qualitative temperature profiles were strikingly similar. Differences in the chemistry of product formation and product reactivity have not been elucidated. Azobenzene required Ni catalyst for effective conversion to NH_3. This pyrolytic selectivity of the simple reductive mode for urea derivatives has proven to be an advantage in distinguishing between barbiturates and other drugs commonly encountered in biological extracts[16].

Temperature profiling of barbiturates revealed that peak tailing was temperature-dependent and was apparently due to a furnace phenomenon (Figs. 11 and 12). When these data were obtained and analyzed graphically, they allowed a better choice of a furnace temperature consistent with required sensitivity and effective GLC–ElCD resolution.

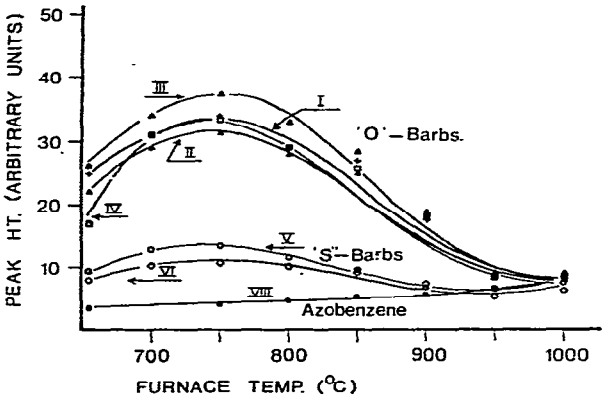

Fig. 10. EICD furnace temperature profiles for barbiturates and azobenzene in the reductive mode.

Methaqualone

Although there is a carbonyl adjacent to a ring nitrogen, Ni catalyst was required for effective conversion to NH_3 under reductive furnace conditions. The profiling of temperature-dependent phenomena are summarized in Fig. 13. An actual MDQ of 125 pg of methaqualone was obtained using a well conditioned OV-17 column.

Compared to the simple reductive mode, peak tailing in the catalytic-reductive mode did not change as dramatically between 700–900° and peak height or peak area response curves usually plateau at 800° furnace temperature. Detector selectivity *vs.* relative standards depended on the mechanism of decomposition of the relative standard and the reactivity of the furnace chemistry mode. EICD N/C selectivity for methaqualone *vs.* *n*-octadecane was $> 10^6$ regardless of furnace temper-

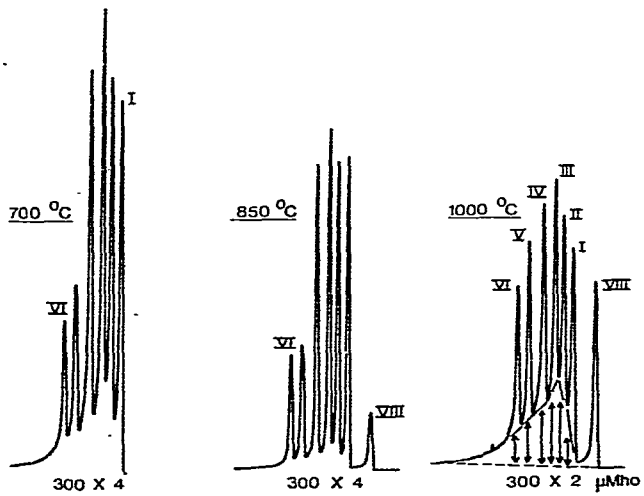

Fig. 11. GLC–EICD chromatograms of barbiturate analyses in the reductive mode with different furnace temperatures.

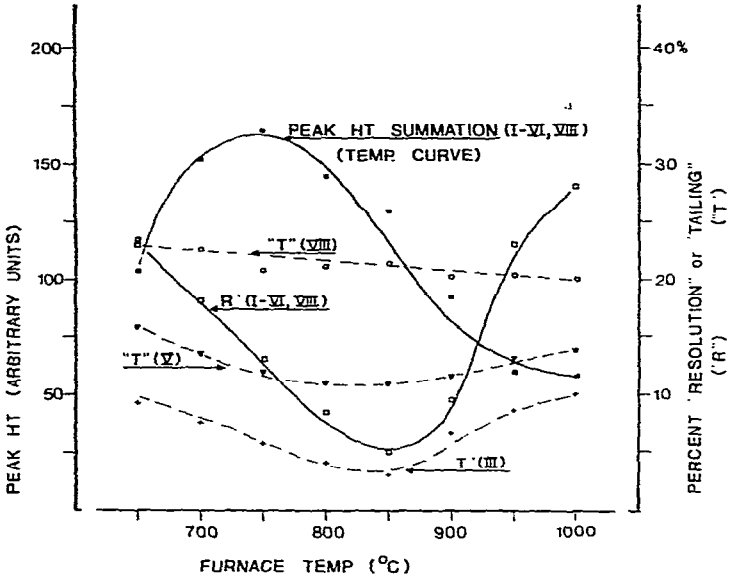

Fig. 12. Temperature profiling of detector response phenomena for barbiturate analysis in the reductive mode at different furnace temperatures.

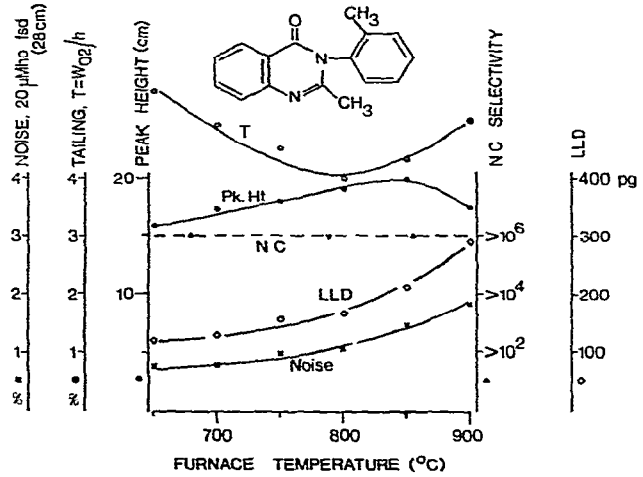

Fig. 13. Temperature profiling of detector response phenomena for methaqualone analysis in the catalytic-reductive mode at different furnace temperatures.

ature, while selectivity *vs.* C_{21} methyl ester and C_{21} hydroxy methyl ester noticeably improved at higher furnace temperatures. The GLC–ElCD analysis of compounds in biological or environmental samples should be profiled to obtain furnace chemistry conditions which contribute to greatest analytical selectivity.

Post-furnace neutralization reaction

Although most reports of ElCD response focus on the furnace chemistry

process or conductivity phenomena, reactive processes may also occur in the post-furnace transfer line (Fig. 14). Using a series of "staggered" injections, detector response to azobenzene was related to the weight of salicylate injected on-column, to the difference in GLC retention time between salicylate and azobenzene, and to the presence or absence of post-furnace $Sr(OH)_2$ abstractor. These phenomena suggested the operation of a post-furnace neutralization reaction involving NH_3 and salicylate, or some acidic pyrolysis product of salicylate. The acidic reactant is relatively non-volatile, based on the observed peak tailing with salicylate alone and the presence of a neutralization reaction at the azobenzene peak.

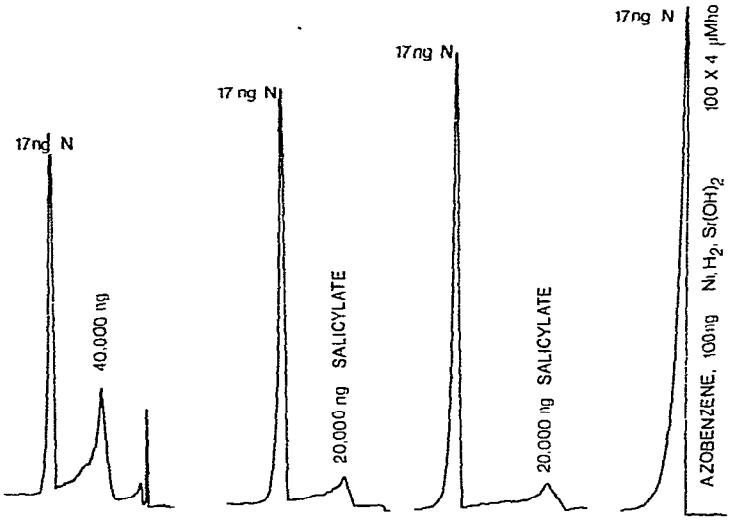

Fig. 14. An illustration of a post-furnace chemical reaction between salicylate and NH_3.

The N/C element-selectivity ratio for azobenzene *vs.* salicylate varied from *ca.* 3500 to < 1000 under different experimental conditions. Selectivity ratio was improved by increasing furnace temperature, adding more Ni catalyst, and increasing furnace residence time. These changes resulted in the more effective reductive decomposition of salicylate.

The determination of selectivity ratios is most often accomplished in one of two ways: (1) the injection of a much larger quantity of relative standard and the direct comparison of peak areas for compound *vs.* relative standard; or (2) the injecton of similar quantities of compound and relative standard and the attenuation (increase) of the detector signal to amplify the detector response to the relative standard, thus allowing the comparison of peak areas after correction for attenuation change. Although sometimes more convenient, the latter approach does not allow an investigation of interference due to catalyst deactivation, inefficient post-furnace abstraction, or post-furnace reaction processes.

Specialized applications and studies

The ability to modify easily furnace chemistry conditions and the selectability of the post-furnace abstractor and conductivity cell for specific reaction products

allow the ElCD to be used as a powerful analytical tool in catalysis research. The reaction-gas manifold can be modified to allow the measured introduction of simple reaction gases (*e.g.*, He, H_2, O_2, etc.), radical initiators such as low-molecular-weight chlorinated hydrocarbons[25], or reaction-gas mixtures. The ability to easily change reaction catalyst or reaction tube offers advantages not always present in static or flow-through reaction chambers[26–29]. As a monitor of product formation, the application of the conductivity cell to studies of deamination, dechlorination, or desulfurization is straightforward. GLC may also serve as an effective and automated system to introduce compounds for qualitative and quantitative screening of catalytic reactivity. Indeed, vapor-phase photochemical reactions involving chlorination–dechlorination mechanisms might be monitored using the quartz reaction tube as the photochemical reaction chamber and the conductivity cell as a selective detector[30].

The identification of furnace chemistry reaction products is sorely lacking, and would surely help in explaining the reaction mechanisms which contribute to detector response. Although it is generally assumed that the major reactive product in the N-selective catalytic-reductive furnace chemistry mode is NH_3, there is no good evidence to exclude alkylamines[19] as important reaction products [λ^0 for $CH_3NH_3^+$, $(CH_3)_2NH_2^+$, $(CH_3)_3NH^+ \approx 58$, 52, and 47 Ω^{-1} cm^2 equiv.$^{-1}$ in water, respectively][12]. Interfacing the ElCD post-furnace transfer line with a chemical-ionization mass spectrometer might provide a selective method of studying product formation as well as the thermodynamics of furnace chemistry processes. Ingram and coworkers have utilized mass spectrometry (MS) in the identification of pyrolytic decomposition products[31–33]. Stable isotope analysis of the post-furnace effluent using combined ElCD–MS could easily be applied to mechanistic studies of selective catalysis (*e.g.*, haloalkane hydrogenolysis *vs.* dehydrohalogenation using deuterium incorporation)[34].

Element-selective gas chromatographic detectors may also find expanded application in the selective GLC profiling of conjugated drug metabolites, an area which has traditionally required the detector selectivity only possible with MS[35–37]. This type of chromatographic profiling by GLC–ElCD would involve selective derivatization with reagents containing N, Cl, S, etc., and the elucidation of selective GLC patterns which could be initially confirmed by MS. Such an approach is certainly limited to selected problems; but, nevertheless, merits consideration in view of the high cost associated with the use of GLC–MS–computer systems for routinized analyses.

CONCLUSIONS

The ElCD represents a unique application of electrochemical detection which allows the selective and sensitive detection of N-containing compounds. Detector sensitivity and selectivity are a result of at least three parameters: thermal decomposition, gas-phase or solid-phase reaction-abstraction, and electrochemical conductance. The understanding of anomalies in detector response characteristics as well as the effective optimization of GLC–ElCD as an analytical tool require that detector parameters, processes, and effects are understood in physical-chemical terms. With an adequate understanding of the principles of ElCD, the application of the ElCD as an analytical tool becomes ever more exciting.

ACKNOWLEDGEMENT

One of the authors (B. E. P.) gratefully acknowledges the continued interests of Tracor Inc. in the application of selective detectors in analytical toxicology.

REFERENCE

1 O. Piringer and M. Pasçalău, *J. Chromatogr.*, 8 (1962) 410.
2 D. M. Coulson, *J. Gas Chromatogr.*, 3 (1965) 134.
3 D. M. Coulson, *J. Gas Chromatogr.*, 5 (1966) 285.
4 P. Jones and G. Nickless, *J. Chromatogr.*, 73 (1972) 19.
5 J. W. Dolan and R. C. Hall, *Anal. Chem.*, 45 (1973) 2198.
6 J. F. Lawrence and A. H. Moore, *Anal. Chem.*, 46 (1974) 755.
7 M. L. Selucky, *Chromatographia*, 5 (1972) 359.
8 D. J. David, *Gas Chromatographic Detectors*, Wiley, New York, 1974, pp. 194–230.
9 J. Ševčík, *Detectors in Gas Chromatography*, Elsevier, Amsterdam, Oxford, New York, 1976, pp. 181–188.
10 R. C. Hall, *J. Chromatogr. Sci.*, 12 (1974) 152.
11 *Model 310 (710) Hall electrolytic conductivity detector*, Tracor, Austin, Texas, 1975.
12 V. E. Bower, R. G. Bates and R. P. Frankenthal, in L. Meites (Editor), *Handbook of Analytical Chemistry*, McGraw-Hill, New York, 1st ed., 1963, pp. 1-20–1-27 and 5-30–5-34.
13 R. C. Hall, personal communication.
14 R. C. Hall and C. A. Risk, *J. Chromatogr. Sci.*, 13 (1975) 519.
15 B. J. Gudzinowicz, *Gas Chromatographic Analysis of Drugs and Pesticides*, Marcel Dekker, New York, 1967, pp. 183–226.
16 B. E. Pape, *Clin. Chem.*, 22 (1976) 739.
17 D. M. Hailey, A. G. Howard and G. Nickless, *J. Chromatogr.*, 100 (1974) 49.
18 I. Mochida, Y. Anju, A. Kato and T. Seiyama, *J. Org. Chem.*, 39 (1974) 3785.
19 R. A. Moss, *Chem. Eng. News*, 49 (1971) 28.
20 D. N. Bailey and P. I. Jatlow, *Clin. Chem.*, 22 (1976) 777.
21 J. T. Biggs, W. H. Holland, S. Chang, P. P. Hipps and W. R. Sherman, *J. Pharm. Sci.*, 65 (1976) 261.
22 B. E. Pape, unpublished data.
23 P. S. Harris, R. T. K. Baker and R. A. Birch, *Carbon*, 11 (1973) 531.
24 L. S. Lobo, D. L. Trimm and J. L. Figueiredo, *Catalysis*, 2 (1973) 1125.
25 A. H. Weiss, B. S. Gambhir and R. B. Leon, *J. Catal.*, 22 (1971) 245.
26 I. Mochida, Y. Anju, H. Yamamoto, A. Kato and T. Seiyama, *Bull. Chem. Soc. Jap.*, 44 (1971) 3305.
27 Y. Anju, I. Mochida, H. Yamamoto, A. Kato and T. Seiyama, *Bull. Chem. Soc. Jap.*, 45 (1972) 2319.
28 I. Mochida, Y. Anju, A. Kato and T. Seiyama, *Bull. Chem. Soc. Jap.*, 45 (1972) 1635.
29 Y. Anju, I. Mochida, A. Kato and T. Seiyama, *Bull. Chem. Soc. Jap.*, 46 (1973) 2593.
30 G. Huybrechts, J. Katihabwa, G. Martens, M. Nejszaten and J. Olbrechts, *Bull. Soc. Chim. Belg.*, 81 (1972) 67.
31 R. Belcher, G. Ingram and J. R. Majer, *Microchem. J.*, 19 (1974) 191.
32 B. C. Capelin, G. Ingram and J. Kokolis, *Microchem. J.*, 19 (1974) 229.
33 G. Ingram and S. M. H. Rizvi, *Microchem. J.*, 19 (1974) 253.
34 I. Matsuzaki, R. L. Burwell, Jr. and T. Nakajima, *J. Catal.*, 13 (1969) 404.
35 S. Billets, P. S. Lietman and C. Fenselau, *J. Med. Chem.*, 16 (1973) 30.
36 R. M. Thompson, N. Gerber, R. A. Seibert and D. M. Desiderio, *Drug Metab. Dispos.*, 1 (1973) 489.
37 D. E. Drayer, J. M. Strong, B. Jones, A. Sandler and M. M. Reidenberg, *Drug Metab. Dispos.*, 2 (1974) 499.
38 A. C. Moffat, *J. Chromatogr.*, 113 (1975) 69.
39 L. Kazyak and R. Permisohn, *J. Forensic Sci.*, 15 (1970) 346.